Article ID: 1000-7032(2009)04-0447-06

Electron Raman Scattering in Spherical Quantum Dots

SUN Hai-chao, ZHANG Yu-qin, LIU Cui-hong*

(*Department of Physics, College of Physics and Electronic Engineering, Guangzhou University, Guangzhong* 510006, *China*)

Abstract: The differential cross-section (DCS) for electron Raman scattering (ERS) in a semiconductor spherical quantum dots was presented. The process of ERS neglects the phonon-assisted transcription and the electron states were confined with GaAs or CdS quantum dot system. Single parabolic conduction and valence bands were assumed. The contribution caused by electron and hole was contrasted separately. The selection rules for the process were also studied. Singularities in the spectra are interpreted for various quantum sizes and different incident photon energies.

Key words: quantum dot; raman scattering; differential cross-section.

CLC number: O472 **PACS**: 78.30.-j; 78.67.Hc **PACC**: 7830 **Document code**: A

1 Introduction

Due to the beneficial effects of strong confinement, there has been enormous activity in studying the growth and electronic configunation, as well as magnetic and optical properties of quantum dots, quantum wires and quantum wells. As one of the most important system in these low-dimensional quantum structures, much work has been done for quantum dots by many scholars[1~7]. In recent years, some researchers have succeeded in preparation of some special quantum dot structures by taking advantage of the technique of semiconductor microelectron and the method of growing without orientation, this quantum dots represent a controllable behavior in quantum energy state and physical behavior. Now, InAs quantum dots have been generated by method of Stransk-Krastanor(S-K) and quantum dots have been made in the ways of original alternate supply(ALS)[8~11]. Otherwise, with the improving of the device such as quantum transistors, high-speed memory elements and infrared photodetectors, quantum dots exhibit more strongpoints than quantum wells and quantum wires do[12~14].

Owing to no-damage and little value of material, ERS has been a widespread way to study semiconductor structure, behavior of phonon and electron[15~20]. With the headway of the microscope electron Raman scattering, we can acquire direct information in the energy band structure and various physical properties of low-dimensional semiconductor systems. Zhang[21] studied Raman scattering in low-dimensional nanostructures and the experimental results showed the dependence of Raman scattering on the phonon modes and the quantum sizes.

Studies of the electron Raman scattering with multiphonon, one phonon or without phonon have been done [22~25]. Our group have studied the ERS with one phonon or without phonon in cylindrical quantum wires and quantum wells[6,24,26], we all got the result that the differential cross-section (DCS) for ERS has an inseparable relation with the sizes of quantum structures. However, we have not paid attention to the different effect between hole and electron for Raman scattering in the spherical quantum dots. In this work, we discussed DCS of ERS without phonon and revealed the distinction effect between hole and electron in the GaAs and CdS

Received date: 2008-11-10; **Revised date**: 2009-05-07

Foundation item: This work is supported by Guangdong Provincial Nature Science Foundation of China (0500187)

Biography: SUN Hai-chao, born in 1983, male, Guangdong Province. His work focus on Raman scatting in low-dimensional system. E-mail: haichaosun@163.com

*: Corresponding Author; E-mail: chliu64@yahoo.com.cn

quantum dots.

In Section 2, the model and the fundamental theory were presented. In Section 3, the expression of the Raman scattering DCS is studied. In Section 4, the numerical results of GaAs and CdS quantum dot were performed and the discussion was showed. In Section 5, the conclusion was given.

2 Model and Theory

We consider a spherical quantum dot with the infinite potential barriers and the radius R_0. The wave functions can be written as follow [27]:

$$\psi_j = Y_{l_j,m_j}(\theta,\varphi)R_{n_j,l_j}(r) \tag{1}$$

with

$$R_{n_j,l_j}(r) = \sqrt{\frac{2}{R_0^3}}\frac{J_{l_j}\left(\chi_{n_j,l_j}\frac{r}{R_0}\right)}{J_{l_j+1}(\chi_{n_j,l_j})} \tag{2}$$

where $j=1,2$ denotes the electron and hole. $Y_{l_j,m_j}(\theta,\varphi)$ are the spherical harmonics functions, they order by l_j and m_j. $J_{l_j}(\chi_{n_j,l_j})$, are the spherical Bessel functions and order by n_j. The quantum numbers: $n_j=1,2,3\cdots$; $l_j=1,2,3\cdots$; $-l_j<m_j<l_j$. Boundary qualification is:

$$J_{l_j}\left(\chi_{n_j,l_j}\frac{r}{R_0}\right)_{r=R_0} = 0 \tag{3}$$

The electron energy levels can be given by:

$$E_{n_j,l_j} = \frac{\hbar^2\chi_{n_j,l_j}}{2m_j^* R_0^2} \tag{4}$$

where m_j^* means the effective mass of electron or hole.

3 Differential Cross-section

The Raman differential cross-section for ERS denotation is expressed as follow[28]:

$$\frac{\mathrm{d}^2\sigma}{\mathrm{d}\Omega\mathrm{d}\omega_s} = \frac{V^2\omega_s^2\eta(\omega_s)}{8\pi^3c^4\eta(\omega_l)}W(\omega_s,\boldsymbol{e}_s) \tag{5}$$

where $\boldsymbol{e}_s$ is the polarization vector for the emitted second radiation field, c is light velocity in vacuum, ω_s is the secondary radiation frequency and ω_l is the frequency of the incident radiation, $\eta(\omega)$ is refraction index as a function of the radiation frequency. $W(\omega_s, \boldsymbol{e}_s)$ is the transition rate calculated according to:

$$W(\omega_s,\boldsymbol{e}_s) = \frac{2\pi}{\hbar}\sum_f |M_j|^2\delta(E_f-E_i) \tag{6}$$

with

$$M_j = \sum_a \frac{\langle f|H_{js}|a\rangle\langle a|H_{jl}|i\rangle}{E_i-E_a+i\Gamma_a} + \sum_b \frac{\langle f|H_{jl}|b\rangle\langle b|H_{js}|i\rangle}{E_i-E_b+i\Gamma_b} \tag{7}$$

where $|i\rangle$ and $|f\rangle$ signify the initial and final states with their corresponding energies E_i and E_f in the quantum dots. $|a\rangle$ and $|b\rangle$ are the intermediate states with their energies E_a and E_b. Γ_a and Γ_b are the corresponding lifetime widths. The Hamiltonian H_{jl} denotes the interaction between electron and the incident radiation. Simultaneously, the Hamiltonian H_{js} describes the interaction between electron and the secondary-radiation field. Utilizing the dipole approximation, the H_{jl} is expressed as follow:

$$H_{jl} = \frac{|e|}{m_0}\sqrt{\frac{2\pi\hbar}{V\omega_l}}\boldsymbol{e}_l\boldsymbol{p} \tag{8}$$

with $\boldsymbol{p} = -ih\nabla$ and $j=1, 2$, where m_0 is the free-electron mass, and the H_{js} is expressed as:

$$H_{js} = \frac{|e|}{m_j}\sqrt{\frac{2\pi\hbar}{V\omega_s}}\boldsymbol{e}_l\boldsymbol{p} \tag{9}$$

This Hamiltonian describes the photon emitted by the electron (hole) in the transition between conduction (valence) subbands in the system. With accounting the intermediate state possible in different bands, we can describe the processes of ERS as such two situations:

(1) Firstly, we consider the intermediate state in conduction band. The system absorbed an incident photon and start up an electron-hole pair with the state $|n_h,l_h\rangle$ in the valence band and the state $|n_e',l_e'\rangle$ in the conduction band. Then, with the electronic transition from the state $|n_e',l_e'\rangle$ to the $|n_e,l_e\rangle$, a scattered photon is generated.

(2) Secondly, we assume the intermediate state in valence band. When one electron jump from the state $|n_h',l_h'\rangle$ to the state $|n_e,l_e\rangle$ with the system absorbs an incident photon, other electron jumps from the state $|n_h,l_h\rangle$ to the state $|n_h',l_h'\rangle$ simultaneously. Overall, we can account the ERS skip process is from the state $|n_h,l_h\rangle$ to state $|n_e,l_e\rangle$.

Consider the $|i\rangle$ includes vacant conduction band, a totally occupied valence band and an incident photon of energy $\hbar\omega_l$, so:

$$E_i = \hbar\omega_l \tag{10}$$

The final state $|f\rangle$ involves an electron-hole pair in a real state and a scattered light with energy $\hbar\omega_s$, thus:

$$E_f = \hbar\omega_s + E_{n_h,l_h} + E_{n_e,l_e} + E_g \tag{11}$$

where E_{n_h,l_h} and E_{n_e,l_e} are determined by Eq. (4). Using energy and momentum conservation laws, we can obtain:

$$E_i - E_a = E_{n_e,l_e} - E_{n'_e,l'_e} + \hbar\omega_s \tag{12}$$

$$E_i - E_b = E_{n'_h,l'_h} - E_{n_h,l_h} + \hbar\omega_s \tag{13}$$

If we just premeditate the backscattering configuration $X(ZZ)\overline{X}$ (The backscattering configuration means the incident radiation wave vector and the scattered radiation wave vector are parallel to a straight line but with opposite direction, both the polarizations of incident and the scattered radiation wave vectors are plumb to the direction of the incident radiation wave vector), on account of the selection $l_e = l_h$ and the Eq. (12) or Eq. (13), the ω_s can be expressed as:

$$\omega_s = \frac{E_{n'_e,l'_e} - E_{n_e,l_e}}{\hbar} \tag{14}$$

or:

$$\omega_s = \frac{E_{n'_h,l'_h} - E_{n_h,l_h}}{\hbar} \tag{15}$$

Next, we perform the DCS matrix elements. Considering electron transition between conduction and valence band, with the envelope function approximation, the $\langle a | H_{jl} | i\rangle$ can be represented as:

$$\langle a | H_{jl} | i\rangle = \frac{i | e | m_a}{R_0^3 m_0}\sqrt{\frac{8\pi}{\hbar V\omega_l}} L_0 W_{i,a} \cdot \int_0^{R_0} \frac{J_l\left(\chi_{n'_e,l}\frac{r}{R_0}\right) J_l\left(\chi_{n_h,l}\frac{r}{R_0}\right)}{J_{l+1}(\chi_{n'_e,l}) J_{l+1}(\chi_{n_h,l})} r^3 \mathrm{d}r \tag{16}$$

And the electron-secondary radiation interaction matrix element $\langle f | H_{jl} | a\rangle$ can be written as:

$$\langle f | H_{js} | a\rangle = \frac{i | e |}{R_0^3}\sqrt{\frac{8\pi}{\hbar V\omega_s}} L_0 W_{a,f} \cdot \int_0^{R_0} \frac{J_l\left(\chi_{n'_e,l}\frac{r}{R_0}\right) J_l\left(\chi_{n_e,l}\frac{r}{R_0}\right)}{J_{l+1}(\chi_{n'_e,l}) J_{l+1}(\chi_{n_e,l})} r^3 \mathrm{d}r \tag{17}$$

By the Eqs. (5) ~ (7), Eq. (1) and Eq. (17), we state the DCS for ERS as:

$$\frac{\mathrm{d}^2\sigma}{\mathrm{d}\Omega \mathrm{d}\omega_s} = \frac{16 e^4 L_0^4 m_a^2 \omega_s \eta(\omega_s)}{\hbar^3 c^4 R_0^{12} m_0^2 \omega_l \eta(\omega_l)} \cdot \frac{| W_{i,a} |^2 | W_{a,f} |^2}{(E_a - E_i)^2 + \Gamma_a} | G_{i,a} |^2 | G_{a,f} |^2 \tag{18}$$

where

$$L_0 = \frac{2l + l!}{(2l+1)!}$$

$$G_{i,a} = \int_0^{R_0} \frac{J_l\left(\chi_{n'_e,l}\frac{r}{R_0}\right) J_l\left(\chi_{n_h,l}\frac{r}{R_0}\right)}{J_{l+1}(\chi_{n'_e,l}) J_{l+1}(\chi_{n_h,l})} r^3 \mathrm{d}r$$

$$G_{a,j} = \int_0^{R_0} \frac{J_1\left(\chi_{n'_e,l}\frac{r}{R_0}\right) J_l\left(\chi_{n_e,l}\frac{r}{R_0}\right)}{J_{l+1}(\chi_{n'_e,l}) J_{l+1}(\chi_{n_e,l})} r^3 \mathrm{d}r$$

$$W_{i,a} = \frac{\hbar^2 \chi_{n'_e,l}^2}{2m_e^* R_0^2} - \frac{\hbar^2 \chi_{n_h,l}^2}{2m_h^* R_0^2}$$

$$W_{a,f} = \frac{\hbar^2}{2m_e^* R_0^2}(\chi_{n_e,l}^2 - \chi_{n'_e,l}^2)$$

Now, we get the matrix elements and the expression of DSC for ERS with the intermediate states in conduction band. Thus, the expressions with intermediate state in valence band have similar form.

4 Results and Discussion

We calculate the DCS for an ERS process without phonon. Considering the system of the GaAs and CdS quantum dots, the physical parameters are adopted as: $m_e^* = 0.067 m_0$, $m_h^* = 0.45 m_0$ for GaAs and $m_e^* = 0.18 m_0$, $m_h^* = 0.51 m_0$ for CdS. $\Gamma_a = 1$ meV $= \Gamma_b$. With fixed the quantum numbers: $l_e = l_h = 0 = l'_e = l'_h$, we can acquired that the ERS process with the intermediate state in the conduction band is just dominated by $v_e(n_h, n'_e, n_e)$, and $v_h(n_e, n'_h, n_h)$ stand for the ERS process with the intermediate state on the valence band.

In Fig. 1, we give the emission spectra for the quantum dots in the $X(ZZ)\overline{X}$ scattering configuration with different materials and various radiuses. The incident radiation energy is $E_L = 3.02$ eV in the Fig. 1(a) and $E_L = 6.81$ eV in the Fig. 1(b). The Fig. 1(a) shows that the DCS of Raman scattering is larger while the size of quantum dot is smaller both in the GaAs and CdS materials . This accords with the Fig. 1. in the Ref. [25], and it is due to quantum dot-size-selective Raman scattering which originates from Ref. [29]. Moreover, the GaAs get stronger effect than CdS in process of ERS. We can

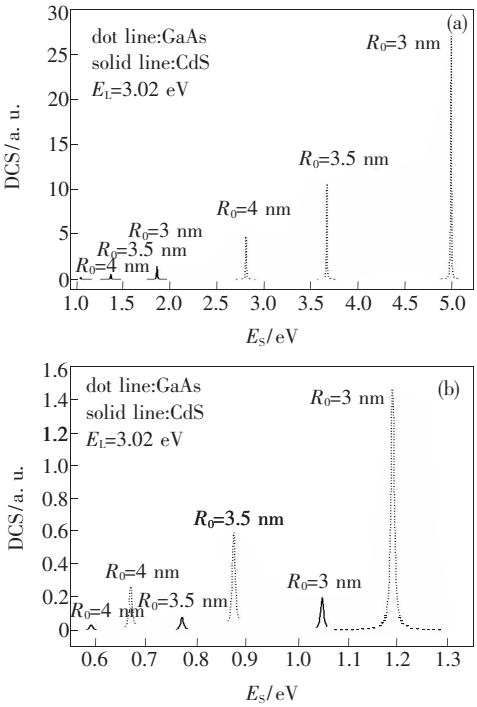

Fig. 1 The Raman DCS for GaAs and CdS quantum dots with various radius in the scattering configuration for electron (a) and for hole (b)

get similar conclusion in the Fig. 1(b), it shows the influence caused by the hole in valence band.

Comparing Fig. 1(a) and Fig. 1(b), we can observe that both the hole and electron all have configuration for Raman scattering DCS, even though, the contribution of electron is much larger than that of the hole. The smaller size the quantum dots have, the more the configuration represents. It agrees with the result in the Ref. [26].

In Fig. 2 we show the emission spectra for the quantum dots in the $X(ZZ)\bar{X}$ scattering configuration with various incident radiation energies in GaAs material. We set the radius $R_0 = 3$ nm and choose various incident radiation energy as $E_L = 3.65$ eV, 3.92 eV, 4.21 eV in Fig. 2(a), and $E_L = 6.81$ eV, 6.95 eV, 7.07 eV in Fig. 2(b). We can discover that the DCS become small while the incident radiation energy E_L increases in the Fig. 2(a). We also get the similar result in the Fig. 2(b), it shows the configuration is due to hole. Comparing Fig. 2(a) and Fig. 2(b), we can obtain that the hole has a weaker configuration for Raman scattering DCS.

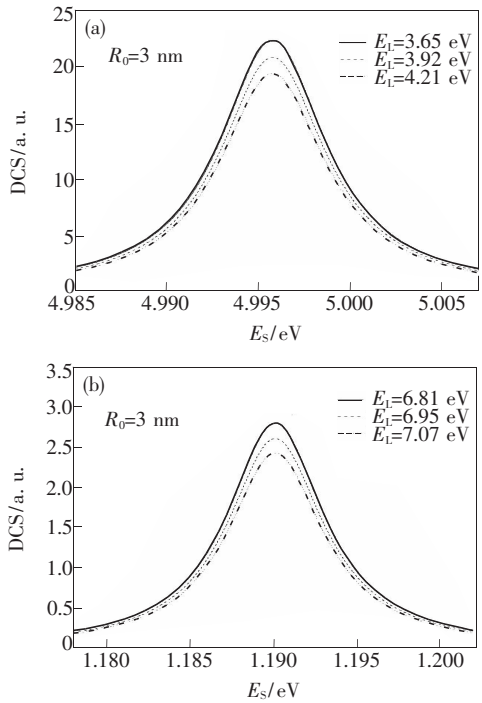

Fig. 2 The Raman DCS for GaAs quantum dots with various incident photon energies in the $X(ZZ)\bar{X}$ scattering configuration for electron (a) and for hole (b)

5 Conclusion

In conclusion, we calculated the DCS of ERS in spherical quantum dots with materials GaAs and CdS. Both electron and hole have contribution to the DCS of ERS, however, the contribution of electron is much larger than that of the hole. The higher incident radiation energy is, the smaller the DCS of ERS is. With the radius becoming smaller, the DCS of ERS tends to larger. We also acquired that the DCS for Raman scattering in GaAs are bigger than that in CdS under the same size and incident radiation energy.

References:

[1] Zhu J L, Chen X. Spectrum and binding of an off-center donor in a spherical quantum dot [J]. *Phys. Rev.* B, 1994, **50**(7): 4497-4502.

[2] Drexler H, Leonard D, Hansen W, *et al.* Spectroscopy of quantum levels in charge-tunable InGaAs quantum dots [J]. *Phys.*

Rev. Lett., 1994, **73**(16):2252-2255.

[3] Empedocles S A, Norris D J, Bawendi M G. Photoluminescence spectroscopy of single CdSe nanocrystallite quantum dots [J]. *Phys. Rev. Lett.*, 1996, **77**(18):3873-3876.

[4] Allan G, Delerue C, Lannoo M. Nature of luminescent surface states of semiconductor nanocrystallites [J]. *Phys. Rev. Lett.*, 1996, **76**(16):2961-2964.

[5] Biasiol G, Kapon E. Mechanisms of self-ordering of quantum nanostructures grown on nonplanar surfaces [J]. *Phys. Rev. Lett.*, 1998, **81**(14):2962-2965.

[6] Zhong Q H, Liu C H. Studies of electronic Raman scattering in CdS/HgS cylindrical quantum dot quantum well structures [J]. *Thin Solid Films*, 2008, **516**(10):3405-3410.

[7] Wang Guanghui, Guo Kangxian. Interband optical absorptions in a parabolic quantum dot [J]. *Phys.* E, 2005, **28**(1):14-21.

[8] Mukai K, Ohtsuka N, Sugawara M, *et al.* Self-formed $In_{0.5}Ga_{0.5}As$ quantum dors on GaAs substrates emitting at 1.3 μm [J]. *Jpn. J. Appl. Phys.*, Part A, 1994, **33**(12):L1710-L1712.

[9] Grundman M, Ledentsov N N, Stier O, *et al.* Excited states in self-organized InAs/GaAs quantum dots: Theory and experiment [J]. *Appl. Phys. Lett.*, 1996, **68**(7):979-981.

[10] Heiz R, Grundman M, Ledentsov N N, *et al.* Multiphonon-relaxation processes in silf-organized InAs/GaAs quantum dots [J]. *Appl. Phys. Lett.*, 1996, **68**(3):361-363.

[11] Mukai K, Shoji H, Sugawara M, *et al.* Phonon bottleneck in self-formed $In_xGa_{1-x}As$/GaAs quantum dots by electroluminescence and time-resolved photoluminescence [J]. *Phys.* B, 1996, **54**(8):R5243-R5246.

[12] Arakawa H, Sakaki H. Multidimensional quantum well laser and temperature dependence of its threshold current [J]. *Appl. Phys. Lett.*, 1982, **40**(11):939-941.

[13] Bimberg D, Grundmann M, Heinrichsdorff F, *et al.* Quantum dot lasers: breakthrough in optoelectronics [J]. *Thin Solid Films*, 2000, **367**(1-2):235-249.

[14] Ranjan V, Singh V A. Shallow-deep transitions of impurities in semiconductor nanostructures [J]. *J. Appl. Phys.*, 2001, **89**(11):6415-6421.

[15] Ismailov T G, Mehdigev B H. Electron Raman scattering in a cylindrical quantum dot in a magnetic field [J]. *Phys.* E, 2006, **31**(1):72-77.

[16] Henry C H, Hopfield J J. Raman scattering by polaritons [J]. *Phys. Rev. Lett.*, 1965, **15**(25):964-966.

[17] Fleury P A, Worlock J M. Electric-field-induced Raman effect in paraelectric crystals [J]. *Phys. Rev. Lett.*, 1967, **18**(16):665-667.

[18] Comas F, Trallero-Giner C, Perez-alvarez R. Interband-interband electronic Raman scattering in semiconductors [J]. *J. Phys.* C, 1986, **19**(32):6479-6488.

[19] Cardona M. Lattice vibrations in semiconductor superlattices [J]. *Superlattices Microstruct.*, 1990, **7**(3):183-192.

[20] Burnett J H, Cheong H M, Westervelt R M, *et al.* Resonant inelastic light scattering in remotely doped wide parabolic GaAs/$Al_xGa_{1-x}As$ quantum wells [J]. *Phys. Rev.* B, 1993, **48**(7):4524-4529.

[21] Zhang S L, Hou Y T, Ho K S, *et al.* Raman selection rules in short-period-superlattice multiple quantum wells [J]. *Phys. Lett.* A, 1994, **186**(5-6):433-437.

[22] Widulle F, Ruf T, Göbel A, *et al.* Raman studies of isotope effects in Si and GaAs [J]. *Phys.* B: *Condensed Matter*, 1999, **263-264**:381-393.

[23] Huang Kun, Zhu Bangfen. Dielectric continuum model and Fröhlich interaction in superlattices [J]. *Phys. Rev.* B, 1998, **38**(18):13377-13386.

[24] Liu C H, Ma B K, Chen C Y. Surface optical phonon-assisted electron Raman scattering in a semiconductor quantum disc [J]. *Chin. Phys.*, 2002, **11**(7):730-736.

[25] Betancourt-Riera R, Betancourt R, Rosas R, *et al.* One phonon resonant Raman scattering in quantum wires and free standing wires [J]. *Phys.* E, 2004, **24**(3-4):257-267.

[26] Zhao Xianfu, Liu Cuihong. Electron Raman scattering in quantum well wires [J]. *Phys.* B,2007, **392**(1-2):11-15.

[27] Chamberlain M P, Trallero-Giner C, Cardona M. Theory of one-phonon Raman scattering in semiconductor microcrystallites [J]. *Phys. Rev.* B, 1995, **51**(3):1680-1693.

[28] Bergues J M, Betancourt-Riera R, Riera R, *et al.* One-phonon-assisted electron Raman scattering in quantum well wires

and free-standing wires [J]. *J. Phys.*: *Condens. Matter.*, 2000, **12**(36):7983-7998.

[29] Tenne D A, Bakarov A K, Torov A I, *et al.* Raman study of self-assembled InAs quantum dots embedded in AlAs: influence of growthtemperature[J]. *Phys.* E, 2002, **13**(2-4):199-202.

球型量子点中的电子拉曼散射

孙海超，张玉芹，刘翠红*

（广州大学 物理电子工程学院，广东 广州 510006）

摘要： 研究了球型半导体量子点中的电子拉曼散射.讨论了初态为导带全满,价带全空时的电子跃迁过程,给出了电子拉曼散射的跃迁选择定则。通过计算 GaAs 和 CdS 材料球型量子点中电子及空穴参与拉曼散射的微分散射截面,分别比较了电子和空穴的不同影响,发现电子对拉曼散射的贡献要远大于空穴的贡献;当选取不同量子点半径时,拉曼散射微分散射截面变化也非常明显;量子点尺寸不变的条件下,改变入射光子能量,可以发现,微分散射截面随入射光子能量增大而减小。

关 键 词： 量子点；拉曼散射；微分散射截面

中图分类号： O472 **PACS：** 78.30.-j；78.67.Hc **PACC：** 7830 **文献标识码：** A

文章编号： 1000-7032(2009)04-0447-06

收稿日期： 2008-11-10；**修订日期：** 2009-05-07

基金项目： 广东省自然科学基金(0500187)资助项目

作者简介： 孙海超(1983－)，男，广东人，主要从事低维量子系统中的拉曼散射研究。
E-mail：haichaosun@163.com

*：通讯联系人；E-mail：chliu64@yahoo.com.cn

重要启示

本刊为方便广大作者的论文进行国际交流,并进一步加快我刊国际化进程,现向广大作者征集相关英语全文写作论文。对专家和编委审查合格的论文,我们将采取优先发表等优惠措施,欢迎广大作者踊跃投寄英语全文写作的学术论文。论文征集范围仍参见《发光学报》征稿简则。

《发光学报》编辑部